Nonlinear reduced order modeling of plasticization cylinders

Tomonori Sadamoto[1], Kenji Kashima[2], Hiroshi Morita[3] and Hiroyuki Mizuno[3]

Abstract— **In this paper, we construct a nonlinear reduced order model of a plasticization cylinder of injection machines, which has a spatially distributed nonlinear dynamics. First, a distributed parameter model for the overall control system is derived based on the physical laws. Next, we attempt to reduce the model complexity focusing on the specific structure of the nonlinearity which arises from temperature-dependency of the rate of heat loss of heaters subjected to natural convection. This enables us to obtain a 28-dimensional model (via an 808-dimensional spatially discretized model) while theoretically guaranteeing a practically satisfactory accuracy. The obtained model is examined experimentally by using a prototype system.**

I. Introduction

Plastic injection molding is a suitable processing method for mass production. Recently, injection molding machines become increasingly important. For example, along with development of a new material such as engineering plastic, lots of metal components such as automotive components are replaced by plastic components for weight reduction. Furthermore, components of IT devices, e.g., chassis, connectors and optical elements are produced by plastic injection molding. In the process of such production, the temperature at plasticization process strongly affects quality of the production. Fig. 1 shows schematic depiction of a plasticization cylinder in charge of the plasticization process. In this process, resin is melted by heat exchange with the internal surface of a barrel heated by bandheaters. Toward quality management and improvement, it is essentially important to simulate and control the plasticization process. To this end, modeling temperature dynamics of the internal surface of the barrel has tremendous potential. Thus, the present paper constructs the dynamical model of a prototype system shown in Fig. 2 based on a theoretic and experimental viewpoint. In particular, since distribution of temperature of the barrel and resin is non-uniform, it is required to carefully model thermal convection and heat exchange with heaters, a water-cooling cylinder and outer air.

In the first half of this paper, we model an overall plasticization cylinder including thermal properties of heaters, radiation to a water-cooling cylinder and outer air. In the previous research [1], the proposed model lacks the accuracy for the purpose above. In particular, it is ignored that the rate of heat loss to the air depends on temperature of heaters [2]. First, we show that the temperature-dependency is not negligible by experiment. Subsequently, we provide a new nonlinear plasticization cylinder model explicitly taking into account the effect. Finally, the obtained model is validated by experiment.

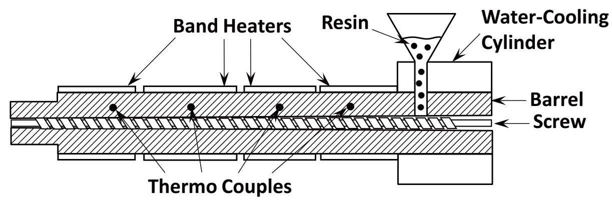

Fig. 1. Schematic depiction of plasticization cylinder.

The obtained model (PDEs or discretized model) is forced to a high dimensional system in general. Thus, it makes difficult to design model-based controllers and observers. Therefore, in the remainder of this paper, we aim to reduce the order of the nonlinear model. However, model order reduction of nonlinear systems is difficult in a general way. Thus, in this paper, we utilize the structure of the nonlinear model arising from radiation to the air. In addition, based on the result in [3], we guarantee not only the stability of the reduced nonlinear system, but also provide a theoretical approximation error bound. As a result, the order is further reduced from 808 to 28 keeping practically satisfactory accuracy.

The organization of this paper is as follows. The plasticization cylinder is modeled in Section II. The first part in Section III is devoted to explaining the configulation of a prototype system shown in Fig. 2 for experiment. In the last part, the obtained model in Section II is validated experimentally. In Section IV-A, we give a theoretical error analysis for the reduced order nonlinear model with a provision of systematic reduction procedure. In Section IV-B, we show a simulation result of the model reduction. Finally, Section V concludes the paper. Proof of the main theorem is described in Appendix.

II. Nonlinear modeling of plasticization cylinders

In Fig. 3, we show the schematic depiction of a two-dimensinal plasticization model consisting of a barrel, outer air, inner fluid, heaters and a water-cooling cylinder. The inner fluid represents melted resin inside the barrel in real injection machines. The water-cooling cylinder has internally a pipe line over the barrel, which cools the barrel by flowing water from IN to OUT shown in Fig. 2. The details of the barrel, the outer air, the water-cooling cylinder and the

[1]Department of Mechanical and Environmental Informatics, Graduate School of Information Science and Engineering, Tokyo Institute of Technology; 2-12-1, Meguro ward, Tokyo

[2]Graduate School of Informatics, Kyoto University; Yoshida Honmachi, Sakyo-ku, Kyoto

[3]Sumitomo Heavy Industries, Ltd; Natsushima, Yokosuka city, Kanagawa

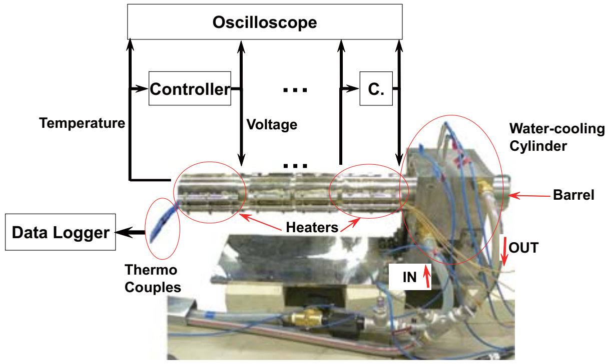

Fig. 2. Prototype system.

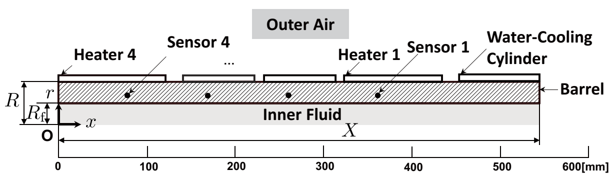

Fig. 3. Schematic of a plasticization cylinder model

inner fluid are described in Section II-A. In addition, the detail model of heaters with the nonnegligible nonlinearity described in Section I are presented in Section II-B. In Section II-C, the overall PDEs are discretized and finally we provide an error system around an equilibrium state.

A. Barrel, Outer air, Inner fluid and Water-cooling cylinder model

In this subsection, we model a barrel, outer air, inner fluid and a water-cooling cylinder. Hereafter, the time variable is t, spatial variables along the longer and radial direction are x and r such as

$$(x, r) \in \mathcal{D} := [0, X] \times [R_{\rm f}, R]$$

with the origin shown in Fig. 3, where X [m] is the length of the barrel, $R_{\rm f}$ and R [m] are internal radius and external radius of the barrel, respectively. In what follows, state variables are

- Temperature of barrel [deg]: $T(t, x, r)$
- Temperature of inner fluid [deg]: $\tilde{T}(t, x)$
- Temperature of the kth heater [deg]: $H_k(t), \quad k = 1, \dots, N$

where N denotes the number of heaters. Note that we here assumed that $\tilde{T}$ (resp. H_k) does not depend on r (resp. x, r). In addition, in view of a preliminary experiment, the temperatures of outer air and a water-cooling cylinder are regarded constant and denoted as $T_{\rm o}$ [deg] and $T_{\rm c}$ [deg], respectively.

First, heat transfer property of a barrel is described by a cylindrical coordinate diffusion equation[1] as

$$\frac{\partial T}{\partial t} = \alpha \left(\frac{\partial^2 T}{\partial r^2} + \frac{1}{r}\frac{\partial T}{\partial r} + \frac{\partial^2 T}{\partial x^2} \right), \quad (x, r) \in \mathrm{int}(\mathcal{D}), \quad (1)$$

[1] $\partial\mathcal{D}$ is the border of $\mathcal{D}$, $\mathrm{int}(\mathcal{D})$ is the inside of $\mathcal{D}$, $\mathbf{n}$ denotes a normal unit vector to $\partial\mathcal{D}$.

where α [m^2/s] denotes a diffusion coefficient. Heat budget on the surface of the barrel is given as Neumann type boundary conditions:

$$-\beta\frac{\partial T}{\partial \mathbf{n}} = h_\bullet(T_\bullet - T), \quad (x, r) \in \mathcal{S}_\bullet, \ \bullet = \{\mathrm{o}, \mathrm{c}\} \quad (2)$$

where β [W/(mK)] denotes the coefficient of thermal conductivity, $h_\bullet$ [W/(m^{2}K)] denotes the coefficient of heat transfer, $\mathcal{S}_{\rm o}, \mathcal{S}_{\rm c} \subset \partial\mathcal{D}$ are sets of contacts to the outer air and the water-cooling cylinder, respectively. In addition, a boundary condition on the interface of inner fluid over $r = R_{\rm f}$ is given by

$$-\beta\frac{\partial T}{\partial r} = h_{\rm f}(\tilde{T} - T), \quad r = R_{\rm f}, \ x \in (0, X), \quad (3)$$

where $h_{\rm f}$ [W/(m^{2}K)] denotes the coefficient of heat transfer. Similalry, heat budget to the kth heater is

$$-\beta\frac{\partial T}{\partial r} = h_k(H_k - T), \quad r = R, \ x \in \mathcal{X}_k \quad (4)$$

where $\mathcal{X}_k \subset [0, X]$ denotes the set of contacts to the kth heater over $r = R$ and h_k [W/(m^{2}K)] denotes the coefficient of heat transfer at contact points. Second, we assume that the inner fluid remains stationary. Thus, its heat transfer property is given by

$$\frac{\partial \tilde{T}}{\partial t} = \tilde{\alpha}\frac{\partial^2 \tilde{T}}{\partial x^2} + h_{\rm f}(T(x, R_{\rm f}) - \tilde{T}), \ x \in (0, X) \quad (5)$$

where $\tilde{\alpha}$ [m^2/s] denotes the coefficient of thermal conductivity of the inner fluid, the second term in the right-hand side in (5) represents the total thermal flow from the barrel to the inner fluid. Similarly, heat exchange at both ends of the outer air is given by

$$-\beta_{\rm f}\frac{\partial \tilde{T}}{\partial x} = h_{\rm o}(T_{\rm o} - \tilde{T}), \ x = 0, X. \quad (6)$$

where $\beta_{\rm f}$ [W/(mK)] denotes the coefficient of thermal conductivity of the inner fluid. Finally, for output equations, $Y_{\rm d} \in \mathbb{R}^N$ [deg] and $Y \in \mathbb{R}^l$ [deg] denote temperatures measured by N sensors shown in Fig. 3 (called controlling thermo couples) and by other sensors (for measurement). The each element is given by appropriately spatially-weighted integration of T.

B. Model of heaters

As preliminary analysis, we consider a heat transfer $\bar{h}_k$ between the kth heater and outer air. In general, coefficients of heat transfer are not static. It is well-known that the rate of heat loss to the air depends on the temperature differences between a heater and the air under natural convection [2]. Toward the quality management of products, this temperature-dependency is not negligible and incorporated explicitly as follows:

Assumption 1: For each $k \in \{1, \dots, N\}$, the heat transfer coefficient between the kth heater and outer air is given by

$$\bar{h}_k(H_k - T_{\rm o}). \quad (7)$$

where $\bar{h}_k : \mathbb{R} \mapsto \mathbb{R}_+$ is non-decreasing in $\mathbb{R}_{0+}$ and non-increasing in $\mathbb{R}_{0-}$.

Hence, the model of the kth heater is

$$\dot{H}_k = \frac{1}{c_k}\left(\frac{V_k(t)^2}{r_k} - \bar{h}_k(H_k - T_\mathrm{o})\cdot a_k(H_k - T_\mathrm{o})\right.$$
$$\left. -2\pi R\int_{\mathcal{X}_k} h_k(H_k - T(x,R))dx\right), \forall k = \{1,\dots,N\} \quad (8)$$

where c_k [J/K] denotes the heat capacity, r_k [ohm] denotes the impedance, a_k [m^2] denotes the outer area of the heater, $2\pi R|\mathcal{X}_k|$ [m^2] denotes the inner area of the heater and $V_k(t)$ [V] denotes the input voltage. In the right side of (8), the second and third term represent the total thermal flow rate to outer air and the barrel, respectively. Note that the other coefficients of heat transfer $h_\mathrm{o}, h_\mathrm{c}, h_\mathrm{f}$ and h_k are constant because the corresponding temperatures are low or the corresponding area is small.

C. Spatial discretization

We discretize (1)-(6) with steps Δx and Δr for x and r axes by means of standard finite element method [4]. Combining this with (7) and (8) yields the following nonlinear system

$$\begin{cases} \dot{\bar{x}} &=& A\bar{x} + B_v\bar{v} + \bar{b}_1 \\ \bar{y}_\mathrm{d} &=& C_\mathrm{d}\bar{x} \\ \bar{y} &=& C_y\bar{x} \\ \bar{w} &=& C_w\bar{x} + D_w\bar{u} \end{cases} \quad (9)$$

$$\begin{cases} \dot{\bar{z}} &=& \begin{bmatrix} -\frac{1}{c_1}\bar{z}_1\psi_1(\bar{z}_1) \\ \vdots \\ -\frac{1}{c_N}\bar{z}_N\psi_N(\bar{z}_N) \end{bmatrix} + \bar{b}_2 + \bar{w} \\ \bar{v} &=& \bar{z} + T_\mathrm{o}\mathbf{1}_N \end{cases} \quad (10)$$

$$\psi_k(\bar{z}_k) := a_k\bar{h}_k(\bar{z}_k) + 2\pi R|\mathcal{X}_k|h_k. \quad (11)$$

Eq. (9) is a dynamics of the barrel and the inner fluid while (10) and (11) are dynamics of the heaters. The physical meanings of variables are as follows: $\bar{x} \in \mathbb{R}^n$ denotes a vector of spatial discretized temperature T and $\tilde{T}$, $\bar{y}_\mathrm{d} \in \mathbb{R}^N$ denotes partial temperatures of T measured by sensors, $\bar{y} \in \mathbb{R}^l$ denotes partial temperatures of T for evaluation, $\bar{z} := [H_1 - T_\mathrm{o}, \dots, H_N - T_\mathrm{o}]^\mathsf{T} \in \mathbb{R}^N$, $\bar{v} := [H_1, \dots, H_N]^\mathsf{T} \in \mathbb{R}^N$ and $\mathbf{1}_N := [1, \dots, 1]^\mathsf{T} \in \mathbb{R}^N$. Furthermore, $\bar{w} \in \mathbb{R}^N$ denotes a heat quantity to heaters, $\bar{u} \in \mathbb{R}^N$ denotes the applied voltage, i.e., V_k^2. Finally, the first and second term of ψ_k represent radiation to the air and the barrel, respectively. Thus, ψ_k represents the coefficient of whole radiation of the kth heater.

Here, we describe the configulation of controller of injection molding machines. Input to each heater is dispersively determined by the corresponding measured temperature y_d (in details, refer to the following section). Thus, the target of controller is given by a desired output y_d^* of y_d, where y_d^* depends on molding products. In general, nonlinear systems do not necessarily have a unique desired state corresponding to a desired output. However, the following proposition guarantees this unique existence for our case.

***Proposition** 1:* Consider a nonlinear system (9)-(11). If $\begin{bmatrix} A & B_v \\ C_\mathrm{d} & 0 \end{bmatrix}$ is non-singular, then, for any $y_\mathrm{d}^* \in \mathbb{R}^N$ there exist unique equilibrium states and inputs $\bar{x}^*, \bar{v}^*, \bar{u}^*$ satisfying $\bar{y}_\mathrm{d}(t) \equiv y_\mathrm{d}^*$.

Proof: The first and second equations in (9) yields that

$$\begin{bmatrix} -\bar{b}_1 \\ y_\mathrm{d}^* \end{bmatrix} = \begin{bmatrix} A & B_v \\ C_\mathrm{d} & 0 \end{bmatrix}\begin{bmatrix} \bar{x}^* \\ \bar{v}^* \end{bmatrix}. \quad (12)$$

Thus, there only exist $\bar{x}^*$ and $\bar{v}^*$ satisfying (12). Furthermore, we define $z^* := \bar{v}^* - T_o\mathbf{1}_N$, then $\bar{u}^*$ is given by

$$\bar{u}^* = -D_w^{-1}\left(\begin{bmatrix} -z_1^*\psi_k(z_1^*) \\ \vdots \\ -z_N^*\psi_k(z_N^*) \end{bmatrix} + \bar{b}_2 + C_w\bar{x}^*\right).$$

Note that $D_w := \mathrm{diag}\{\frac{1}{c_1r_1}, \dots, \frac{1}{c_Nr_N}\}$ is non-singular. ∎

In the remainder of this section, we rewrite (9)-(11) as an error system from the desired value. Define errors with respect to each variable, e.g., $z := \bar{z} - z^*$, $y := \bar{y} - C_y\bar{x}^*$. From simple calculation,

$$\dot{z} = \begin{bmatrix} -(z_1 + z_1^*)\psi_k(z_1 + z_1^*) \\ \vdots \\ -(z_N + z_N^*)\psi_k(z_N + z_N^*) \end{bmatrix} + C_wx$$
$$+ D_wu + \bar{b}_2 + C_w\bar{x}^* + D_w\bar{u}^*$$

holds. Thus, we have a nonlinear system

$$\begin{cases} \dot{x} &=& Ax + B_vz \\ y_\mathrm{d} &=& C_\mathrm{d}x \\ y &=& C_yx \\ w &=& C_wx + D_wu \end{cases} \quad (13)$$

$$\Sigma_{nl} : \dot{z} = \tilde{\Psi}(z) + w, \quad v = z \quad (14)$$

where

$$\tilde{\Psi}(z) := \left[\tilde{\psi}_k(z_1), \dots, \tilde{\psi}_k(z_N)\right]^\mathsf{T} \in \mathbb{R}^N, \quad \tilde{\Psi}(0) = 0 \quad (15)$$

$$\tilde{\psi}_k(z_k) := -\left((z_k + z_k^*)\psi_k(z_k + z_k^*) - z_k^*\psi_k(z_k^*)\right) \quad (16)$$

and z_k denotes the kth element of z for any $k \in \{1, \dots, N\}$.

III. Experimental Results

In this section, we experimentally validate the nonlinear model derived in the previous section.

A. Schematic of prototype system

Configulations of the prototype system shown in Fig. 2 are as follows: The test object consists of a barrel, $N = 4$ heaters and one water-cooling cylinder. The cylindrical barrel has several thermo couples on its interior wall also implanted several thermo couples (controlling thermo couples) are inside the barrel. Input to each heater is dispersively determined by temperatures measured by the implanted sensors. Note that the number of implanted thermo couples is 4. In addition, sequential data of experiment are sampled by an ocilloscope and a data logger during 30 [min] where sampling interval is short enough.

The nonlinear function of heat transfer $\bar{h}_k(\bar{z}_k)$ in (7) is determined as follows: First, several actual coefficients are identified by experiment. In Fig. 4, we show the resultant

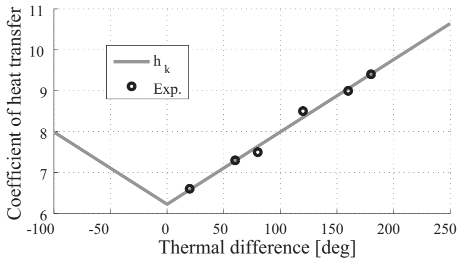

Fig. 4. Coefficients of heat transfer $\bar{h}_k$.

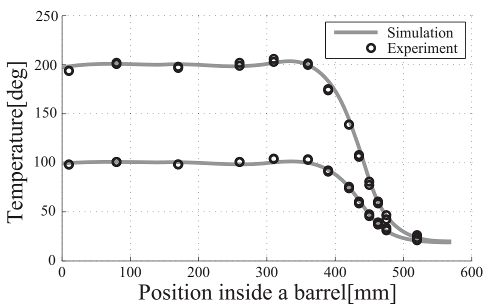

Fig. 5. Steady temperature distribution at some points inside barrel.

coefficients with respect to the first heater as circles. Second, the function $\bar{h}_1(\bar{z}_1)$ is approximately determined by a least square method in $\mathbb{R}_{0+}$ and let $\bar{h}_1(-\bar{z}_1) = \bar{h}_1(\bar{z}_1)$. Since similar experimental results are obtained for the other heaters, we take $\bar{h}_k = \bar{h}_1$ for $k \in \{2, \dots, N\}$. The other parameters, e.g., α in (1), $h_{\rm o}$ and $h_{\rm c}$ in (2), are referred to [2]. Taking $\Delta x = \Delta r = 5$ [mm], we have an 808-dimensional nonlinear model.

B. Model validation

First, we validate steady-state characteristics of the model. Steady temperature distribution inside the barrel obtained by the experiment and simulation are shown in Fig. 5 where the vertical axis indicates temperatures and the horizontal axis indicates positions inside the barrel in Fig. 3. In Fig. 5, we plot experimental results by the circles for the desired temperatures 200 [deg] and 100 [deg], respectively where the two results are plotted in each case. Moreover, the solid lines are simulation results of $\bar{x}^*$ in Proposition 1. This figure shows that the derived model accurately explains experimental results.

Second, we show transient responses obtained by the experiment and simulation as the blue and red lines in Fig. 6. In addition, the solid and dotted lines are for different controlling configurations. Measurement points are shown in Fig. 7 as $Z1$ and $P1$-$P9$. These figures show that the derived model accurately explains experimental results. Therefore, we conclude that an accurate nonlinear model is obtained.

IV. Model Order Reduction

In the preceding section, we showed the validity of the obtained nonlinear model. However, since the dimension of the model is 808, it is not useful for designing controllers and observers. On the other hand, the model obtained by coarser spatial discretization cannot simulate behaviors of the real system. In fact, a 409-dimensional model with the spatial discretization width $\Delta x = 10$ [mm] does not simulate accurately. Thus, in this section, we reduce the dimension of the whole nonlinear system while preserving input-output performances. Since model reduction of general nonlinear systems is challenging, we utilize a specific structure as the low-dimensional nonlinear system is feedback inter-connected to the high-dimensional linear system. We, then, reduce the linear system part only in order to derive a low-dimensional system. The linear system is defined as

$$\Sigma_{lin} : \begin{cases} \dot{x} &= Ax + B_v v \\ y &= C_y x \\ w &= C_w x + D_w u \end{cases} \tag{17}$$

where y denotes an evaluating output in (13) and the overall nonlinear system $\Sigma := (\Sigma_{lin}, \Sigma_{nl})$ is shown in Fig. 8.

Furthermore, let a reduced linear system be $\hat{\Sigma}_{lin}$ and an inter-connected reduced nonlinear model be $\hat{\Sigma} := (\hat{\Sigma}_{lin}, \Sigma_{nl})$.

A. Error analysis

For the following discussion, we assume that matrix A in (17) is Hurwitz. This is the case for our model, since Σ_{lin} is a diffusive system. Thus, a reduced nonlinear model must keep stability with a small approximation error.

As preliminary of main results, we introduce some notations as follows: γ_{ij} is H^∞-norm of G_{ij}, that is a transfer function from $i \in \{y, w\}$ to $j \in \{u, v\}$ of Σ_{lin}. Similary, $\hat{\gamma}_{ij}$ is H^∞-norm of $\hat{G}_{ij}$, that is a transfer function from i to j when $\hat{\Sigma}_{lin}$ is stable. H^∞-norm of an error system $G_{ij} - \hat{G}_{ij}$ is ϵ_{ij}. In addition, we assume that $\hat{\Sigma}_{lin}$ is minimal realization without loss of generality.

***Theorem** 1:* Consider Σ_{nl} in (14) and Σ_{lin} in (17). Define

$$\mu := \max_{k=1,\dots,N} (\mu_k) \tag{18}$$

$$\mu_k := \frac{c_k}{\nu_k} \tag{19}$$

$$\nu_k := \min_{z \in \mathbb{R}^N} \psi_k(z) (= \psi_k(0)). \tag{20}$$

Let $\hat{\Sigma}_{lin}$ be a stable linear system satisfing

$$\hat{\gamma}_{wv} \mu < 1 \tag{21}$$

then the overall reduced order system $\hat{\Sigma} = (\hat{\Sigma}_{lin}, \Sigma_{nl})$ is asymptotically stable. Moreover, upper bound of output error such as $\|y - \hat{y}\|_{\mathcal{L}_2} \le \epsilon \|u\|_{\mathcal{L}_2}$ for any square-integrable input u is given by

$$\epsilon = \frac{\epsilon_{yv} \mu \gamma_{wu}}{1 - \gamma_{wv} \mu} + \frac{\hat{\gamma}_{yv} \mu}{1 - \hat{\gamma}_{wv} \mu} \frac{\epsilon_{wv} \mu \gamma_{wu}}{1 - \gamma_{wv} \mu}. \tag{22}$$

Proof: See Appendix. ■

The parameter μ in (18) and μ_k in (19) act as an incremental gain of nonlinear systems, the details are described in the proof. The parameter μ_k is characterized by the lower value of the coefficient of radiation ψ_k. Since ψ_k dominates the decay rate of energy of heaters, it implies that (22) evaluates

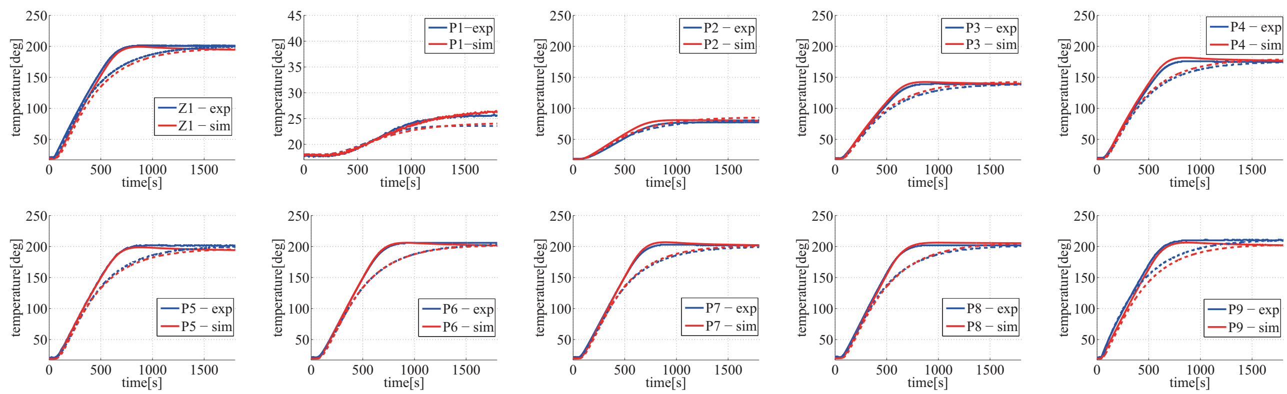

Fig. 6. Transient responses at several measurement points shown in Fig. 7.

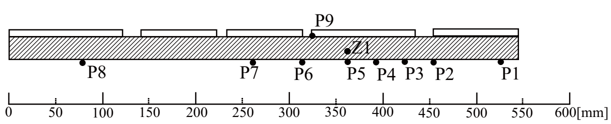

Fig. 7. Measurement points.

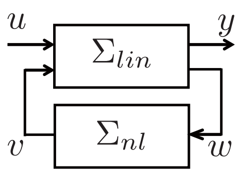

Fig. 8. Overall nonlinear system.

an approximation error with the minimum decay rate. It is reasonable that the error ϵ becomes larger as ψ_k gets smaller.

The reduction procedure using this theorem is as follows: Note that $\epsilon_{ij} \leq \|G - \hat{G}\|_\infty$ holds where G and $\hat{G}$ are transfer functions of Σ_{lin} and $\hat{\Sigma}_{lin}$, respectively. In addition, we define δ satisfying $\epsilon_{ij} \leq \delta$, then $\hat{\gamma}_{ij} \leq \gamma_{ij} + \delta$ holds.

1) For given Σ_{lin} and Σ_{nl}, compute γ_{ij} and μ in (18).
2) Find maximum $\delta > 0$ such that the error bound ϵ in (22) is less than a desired value and (21) holds. Note that we can replace ϵ_{ij} and $\hat{\gamma}_{ij}$ by δ and $\gamma_{ij} + \delta$ as a priori bounds.
3) Find a reduced order model $\hat{\Sigma}_{lin}$ satisfying $\|G - \hat{G}\|_\infty \leq \delta$ by means of a model reduction method with preserving stability, e.g., balanced truncation [5], [6].
4) Obtain $\hat{\Sigma}$ by inter-connecting $\hat{\Sigma}_{lin}$ and Σ_{nl} as shown in Fig. 8.

B. Simulation results

In this subsection, we demonstrate the efficiency of the model reduction method described in the previous subsection. For given Σ_{lin} and Σ_{nl}, we have $\mu = 30.0$, $\gamma_{wu} = 1.3 \times 10^{-4}$, $\gamma_{yv} = 1.7$ and $\gamma_{wv} = 3.2 \times 10^{-2}$. In the second step of the procedure, we have $\delta = 3 \times 10^{-4}$ such that $\epsilon < 1.5 \times 10^{-1}$. Reducing Σ_{lin} by means of balanced truncation, finally, we have a further reduced 28-dimensional nonlinear model compared to the 808-dimensional original model. Since the obtained model satisfies (21) with $\mu\hat{\gamma}_{wv} = 0.96$, the model is stable. This model is the smallest one satisfying the condition in (21). Moreover, the error bound results in $\epsilon = 2.7 \times 10^{-2}$. Taking into account the fact that $y(t)$ and $u(t)$ are $\mathcal{O}(10^3)$ and $\mathcal{O}(10^2)$, we conclude that the model which approximates the original model accurately.

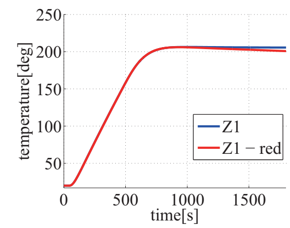

Fig. 9. Comparison of original model with reduced order model.

Similarly to Section III, we show a transient response of the reduced model and the original model shown in Fig. 9, where the input signal is the same as used in model validation. The blue and red lines depict outputs corresponding to the temperature at $Z1$ of the original and reduced order model. This figure shows that we obtained the accurate reduced order model for the spatially distributed nonlinear dynamics.

V. Conclusion

In the first half of this paper, we provided a new nonlinear model for plasticization systems including nonlinear radiation to outer air. Furthermore, constructing a prototype system, we showed the accuracy of the model by experiment. In the latter half, we reduced the order of the nonlinear model with theoretical guarantee about the approximation error. The accuracy of the obtained model was evaluated by comparison with simulation results. Therefore, we concluded that the reduced nonlinear model accurately explains the experimental results.

Appendix

***Definition** 1:* Consider a nonlinear system

$$\dot{x} = f(x, u), \quad y = g(x, u) \tag{23}$$

where $x \in \mathbb{R}^n, u \in \mathbb{R}^m, y \in \mathbb{R}^l$. Suppose that $f(0,0) = 0, g(0,0) = 0$ and $x = 0$ are stable equilibrims. If there exists a bounded function $\beta(p,s) : \mathbb{R}^n \times \mathbb{R}^n \mapsto \mathbb{R}$ such that $\beta(p,s) \geq 0, \beta(0,0) = 0$ and

$$\|y_2 - y_1\|_{2,T}^2 \leq \mu^2 \|u_2 - u_1\|_{2,T}^2 + \beta(x_{1,0}, x_{2,0}) \tag{24}$$

for $u_1, u_2 \in \mathcal{L}_{2,T}^m, \forall T \geq 0$, then the nonlinear system (23) has a $\mathcal{L}_2$-bounded incremental gain μ.

Similarly, an incremental gain for linear system is defined, which results in H^∞-norm.

***Lemma** 1:* Consider the augmented system of a nonlinear system (23) as

$$\Sigma_{\text{aux}} : \begin{cases} \dot{x_1} = f(x_1, u_1), & y_1 = g(x_1, u_1) \\ \dot{x_2} = f(x_2, u_2), & y_2 = g(x_2, u_2) \end{cases} . \tag{25}$$

The fact that a nonlinear system (23) has incremental gain μ is equivalent to that Σ_{aux} is dissipative with a supply rate

$$s(y_1, u_1, y_2, u_2) = \mu^2 |u_2 - u_1|^2 - |y_2 - y_1|^2. \tag{26}$$

Proof: See [7]. ■

***Lemma** 2:* Define $\nu_k > 0$ in (20). If assumption 1 holds and $z_{k,1} \geq z_{k,2}$ is satisfied for all $z_{k,1}, z_{k,2} \in \mathbb{R}$, then

$$z_{k,1}\psi_k(z_{k,1}) - z_{k,2}\psi_k(z_{k,2}) \geq \nu_k (z_{k,1} - z_{k,2}) \tag{27}$$

holds.

Proof: It is obviously proven in the case of $\psi_k(z_{k,1}) = \nu_k$. In what follows, we consider the case of $\psi_k(z_{k,1}) \neq \nu_k$. Then, $z_{k,1}(\psi_k(z_{k,1}) - \nu_k) \geq z_{k,2}(\psi_k(z_{k,2}) - \nu_k)$ is equivalent to

$$z_{k,1} \geq \frac{\psi_k(z_{k,2}) - \nu_k}{\psi_k(z_{k,1}) - \nu_k} z_{k,2}.$$

Assumption 1 yields that $\psi_k(z_{k,1}) \geq \psi_k(z_{k,2})$ holds when $z_{k,1} \geq z_{k,2} \geq 0$. Thus, (27) follows. Similarly to this, we have (27) when $0 > z_{k,1} \geq z_{k,2}$. It is obviously proven in the case of $z_{k,1} \geq 0 \geq z_{k,2}$. Hence, the claim is proven. ■

***Proposition** 2:* Consider a given Σ_{lin} in (17). Let Σ_{lin} be stable and $\hat{\Sigma}_{lin}$ be a stable reduced linear system. In addition, suppose that a given Σ_{nl} in (14) is zero-state detectable while $\hat{\Sigma}_{lin}$ and Σ_{nl} have incremental gain $\hat{\gamma}_{ij}$ and μ. If

$$\gamma_{wv}\mu < 1 \tag{28}$$

holds, then $\Sigma = (\hat{\Sigma}_{lin}, \Sigma_{nl})$ has an incremental gain and is aymptotically stable with zero input. Furthermore, an output error bound ϵ such as $||y - \hat{y}||_{\mathcal{L}_2} \leq \epsilon ||u||_{\mathcal{L}_2}$ is given by

$$\epsilon = \epsilon_{yu} + \frac{\epsilon_{yv}\mu\gamma_{wu}}{1 - \gamma_{wv}\mu} + \frac{\hat{\gamma}_{yv}\mu}{1 - \hat{\gamma}_{wv}\mu}\left(\epsilon_{wu} + \frac{\epsilon_{wv}\mu\gamma_{wu}}{1 - \gamma_{wv}\mu}\right) \tag{29}$$

Proof: See [3]. ■

Proof of theorem 1 : First, we show that a nonlinear scalar system $\dot{z}_{k,1} = \tilde{\psi}_k(z_{k,1}) + w_{k,1}, \ v_{k,1} = z_{k,1}$ has an incremental gain μ_k. To this end, we define a nonlinear system

$$\Sigma_{nl}^{(k)} : \dot{z}_k = \begin{bmatrix} \tilde{\psi}_k(z_{k,1}) \\ \tilde{\psi}_k(z_{k,2}) \end{bmatrix} + w_k, \quad v_k = z_k$$

where $z_k := [z_{k,1}, z_{k,2}]^\mathsf{T}$ and $w_k := [w_{k,1}, w_{k,2}]^\mathsf{T}$. From Lemma 1, we show that $\Sigma_{nl}^{(k)}$ has a storage function $S_k(z_k) := \mu_k(z_{k,1} - z_{k,2})^2$ with a supply rate $s_k(\cdot) = \mu_k^2|w_{k,2} - w_{k,1}|^2 - |v_{k,2} - v_{k,1}|^2$, namely, it suffices to show that

$$\dot{S}_k(z_k) \leq \mu_k^2 |w_{k,2} - w_{k,1}|^2 - |v_{k,2} - v_{k,1}|^2. \tag{30}$$

Lemma 2 for $z_{k,1} \geq z_{k,2}$ yields that

$$\begin{aligned} \dot{S}_k(z_k) &= 2\mu_k(z_{k,1} - z_{k,2})\left(-\frac{1}{c_k}((z_{k,1} + z_k^*)\right. \\ &\quad \psi_k(z_{k,1} + z_k^*) - z_k^*\psi_k(z_k^*) - (z_{k,2} + z_k^*) \\ &\quad \left.\psi_k(z_{k,2} + z_k^*) + z_k^*\psi_k(z_k^*)) + w_{k,1} - w_{k,2}\right) \\ &\leq -\frac{2}{c_k}\mu_k(z_{k,1} - z_{k,2})^2\nu_k + 2\mu_k(z_{k,1} - z_{k,2})(w_{k,1} - w_{k,2}) \end{aligned}$$

holds. Similarly to the case of $z_{k,1} < z_{k,2}$, we see that the sufficient condition for (30) is

$$-\frac{2\mu_k\nu_k}{c_k}p^2 + 2\mu_k pq - \mu_k^2 q^2 + p^2 \leq 0 \tag{31}$$

for any $p, q \in \mathbb{R}$. Eq. (31) is equivalently written as

$$\left(1 - \frac{2\mu_k\nu_k}{c_k}\right)\left(p + \frac{\mu_k c_k}{c_k - 2\mu_k\nu_k}q\right)^2 - \mu_k^2\left(1 + \frac{c_k}{c_k - 2\mu_k\nu_k}\right)q^2 \leq 0. \tag{32}$$

On the other hand, it follows from (19) that

$$c_k - 2\mu_k\nu_k \leq 0, \quad 1 + \frac{c_k}{c_k - 2\mu_k\nu_k} \geq 0.$$

Thus, (31) follows. Therefore, the nonlinear scalar system $\dot{z}_{k,1} = \tilde{\psi}_k(z_{k,1}) + w_{k,1}, \ v_{k,1} = z_{k,1}$ has the incremental gain μ_k. Second, we show that Σ_{nl} has the incremental gain $\mu := \max_k(\mu_k)$. Define

$$S(z_1, \ldots, z_N) := \sum_{k=1}^{N} S_k(z_k). \tag{33}$$

Then, (30) yields that $S(\cdot)$ satisfies

$$\dot{S}(z_1, \ldots, z_N) \leq \mu^2 |w_{:,2} - w_{:,1}|^2 - |v_{:,2} - v_{:,1}|^2$$

where $w_{:,1} := [w_{1,1}, \ldots, w_{N,1}]^\mathsf{T}$. Thus Σ_{nl} has the incremental gain $\mu := \max_k(\mu_k)$. Finally, we show the stability of $\hat{\Sigma}$ and the error bound. Eq. (14) implies that Σ_{nl} is zero-state detectable. Thus, Proposition 2 shows that the overall nonlinear system $\hat{\Sigma}$ is asymptotically stable with zero input. Furthermore, since $\epsilon_{yu} = \epsilon_{wu} = 0$ holds, the error bound is given by (22). ■

References

[1] T. Akashi, "Temperature control of heating cylinder of injection moulding machine by decoupling method," in *Transactions of SICE(in Japanese), 1986.*, vol. 22,No.2. SICE, 1986, pp. 106–113.

[2] J. Holman, *Heat Transfer tenth edition*, ser. McGraw-Hill Series in Mechanical Engineering. McGraw Hill Higher Education, 2009.

[3] B. Besselink, N. Van De Wouw, and H. Nijmeijer, "Model reduction of nonlinear systems with bounded incremental L2 gain," in *Proc. of the 50th IEEE Conference on Decision and Control*, 2011, pp. 7170–7175.

[4] J. Ferziger and M. Perić, *Computational methods for fluid dynamics*. Springer Berlin etc, 1999, vol. 3.

[5] G. Obinata and B. Anderson, *Model reduction for control system design*, ser. Communications and control engineering. Springer, 2000.

[6] A. Antoulas, *Approximation of large-scale dynamical systems*. Society for Industrial Mathematics, 2005, vol. 6.

[7] B. Romanchuk and M. James, "Characterization of the Lp incremental gain for nonlinear systems," in *Proc. of the 35th IEEE Conference on Decision and Control*, 1996, pp. 3270–3275.